Effect of variable thermal conductivity and specific heat capacity on the calculation of the critical metal hydride thickness for Ti1.1CrMn

Mazzucco, Andrea; Rokni, Marvin Mikael

Published in:
Proceedings of the 20th World Hydrogen Energy Conference (WHEC 2014)

Publication date:
2014

Document Version
Peer reviewed version

WHEC 2014
20th World Hydrogen Energy Conference 2014
June 15[Sun] ~ 20[Fri], 2014 KDJ Convention Center, Gwangju Metropolitan City, Korea

Effect of variable thermal conductivity and specific heat capacity on the calculation of the critical metal hydride thickness for $Ti_{1.1}CrMn$

Andrea Mazzucco[a*], Masoud Rokni[a]
[a] Department of Mechanical Engineering, Technical University of Denmark, Denmark

ABSTRACT

High pressure metal hydrides have been recently considered as one of the most promising hydrogen solid storage options for on-board applications.
Unfortunately the high purchasing costs related to these materials and the complexity related to building a scaled high pressure tank system with activated powder and embedded heat exchanger makes difficult to set up experimental facilities. Trustable simulation models that can address the system´s performances to a particular design are then a fundamental step to be taken prior any experimental setup.
This study considers a detailed 1D fueling model is applied to the metal hydride system, with $Ti_{1.1}CrMn$ as the absorbing alloy, to predict the weight fraction of absorbed hydrogen and solid bed temperature. Dependencies of thermal conductivity and specific heat capacity upon pressure and hydrogen content respectively, are accounted for, by interpolating experimental data. The effect of variable parameters on the critical metal hydride thickness is investigated and compared to results obtained from a constant parameter analysis.
At the end, the discrepancy in the metal hydride thickness value is estimated around 10%.

Keywords: Hydrogen solid storage, metal hydrides, 1D numerical model, high-pressure storage tank, heat exchanger

1. Introduction

In the perspective of an energy system based on hydrogen, the fuel cell vehicle (FCV) is expected to be the core of the future transport sector. A major challenge in a hydrogen-fueled vehicle is the design of an efficient storage system, due to low energy density per unit volume of gaseous hydrogen at ambient pressure (approximately 1/3000 of liquid gasoline). As consumers place a high priority on the achievement of an adequate cruising range, it is crucial to compact the storage system and guarantee an adequate amount of stored hydrogen in order to make FCVs attractive for potential customers.

* Corresponding author. Tel.:+45-91945382, E-mail address: andmaz@mek.dtu.dk.

Storage systems based on high-pressure metal hydrides (HPMH) have been recently investigated by car manufacturers with the main aim of enhancing volumetric density and reduce filling times for the next generation of hydrogen vehicles [1], [2].
Combining current high-pressure tanks with adsorbing alloys having high equilibrium pressures can improve the charge/discharge characteristics and the volume density [3]. Main advantages compared to complex metal hydrides are a faster kinetics, the possibility to control the absorption rate by controlling the temperature and cold start capability. Disadvantages of present high pressure intermetallic materials are low gravimetric capacities and low thermal conductivities [4]. Storage systems based on high-pressure metal hydrides (HPMH) are typically

difficult to build and test because of the high pressures involved and the pyrophoric nature of activated powders. In addition, the purchasing cost of these materials makes the storage system relatively expensive even at lab-scale sizes. For this reason it is extremely important to develop reliable computational models that can be applied to full scale systems maintaining a good grade of accuracy and simplicity. The possibility of using a constant parameters model for the metal hydride (MH) would lower the complexity of the calculation, but its accuracy must be investigated. In order to do so, such simple approach is compared with results obtained by implementing variable parameters. Experimental data on thermal conductivity and specific heat capacity have been interpolated with dependencies upon hydrogen pressure and content in the metal hydride bed respectively. At first, the two model cases are compared with respect to temperature and weight fraction of absorbed hydrogen in the MH bed. As the heat exchanger is the key component of the HPMH storage system, the effect of variable parameters on its design is also addressed by comparing the calculated value in the two cases for the critical MH thickness δ, which is here considered as the main design criterion.

For HPMH systems different simulation models have been presented in the literature. However, they all implement metal hydride parameters independent upon the fueling and hydriding conditions.

Raju et al. in ref. [5] presented a 0D model in MatLab/Simulink, which combined ideal and real gases formulation in the transient energy and mass balances under a final internal pressure of 50 MPa. Their study provides information on the heat flow dynamics in the tank with no insight on the heat flow and absorption process behavior.

In ref. [6], Pourpoint et al. expanded their study presented in ref. [7] and developed a basic 3D model in Fluent, integrated with the data acquired from the characterization of thermal properties of $Ti_{1.1}CrMn$ and obtained from testing 100g of material. Results show low agreement between numerical and experimental results. Reasons for that can be identified in the neglect of the transient mass balance, thermal masses of the pressure vessel and thermocouple probe.

Visaria and Mudawar in ref. [8] presented a 1D model to predict the temperature and absorption rate at different distances from the cooling tube. Their model is obtained by applying the heat transfer equation to a general domain, which does not differentiate among gaseous hydrogen, absorbent and solid material and which does not account for the hydrogen mass transfer into the tank.

In further studies the same model was used to design an U-tube and a coiled tube configuration for the heat exchanger [9]–[11]. The model was validated against experimental data for the U-tube plate finned heat exchanger during hydriding in ref. [12] while in ref. [13] they compared the two configurations with regards to the dehydriding process and validated the 3D computational models against measured data.

2. Methodology and model description

2.1 Dymola Software

The simulation software used for deployment of the model is Dymola which is a commercial modeling and simulation environment based on the open Modelica language. The language is a unified object-oriented language for physical system modelling. True ordinary differential and algebraic equations are solved with a non-causal approach. Different incorporated solvers, such as Dassl, Euler, Lsoder, can be used to solve large complex systems. [14].

2.2 High pressure absorbing alloy

The absorbing alloy considered in this study is $Ti_{1.1}CrMn$, a well-known HPMH for which main properties are easy to find in the literature.

Rising attention has been given to such metal hydride in hydrogen storage systems for its high volumetric capacity (~50 g/L) and cold start capability that permits hydrogen desorption even at -30 °C.

However, its relatively low gravimetric capacity (<2 wt% H_2) [15], and high density, make the storage system significantly heavier than most of the other on-board storage solutions. In addition, the poor thermal properties of the metal-hydrogen system make the design of the heat exchanger quite challenging, as it has to efficiently fulfill cooling and heating demands during hydriding and dehydriding respectively.

At the end, it is worth saying that property measurements for such metal hydride are quite challenging due to the high pressures involved and the pyrophoric nature of the activated material.

The nominal values for the MH properties are obtained from ref. [8] and refer to the measurements carried out at the Purdue University Hydrogen Systems Laboratory (HSL).

2.3 Model Setup

The 1D model is used to discretize the domain with a 1 mm step, by the finite temperature difference method in Dymola software. The model considers the evidenced portion of tank presented in Fig. 1, which refers to a U-tube

configuration for the heat exchanger. When the coolant temperature is assumed constant along the tube, only half domain can be considered, as the center line corresponds to an adiabatic boundary.

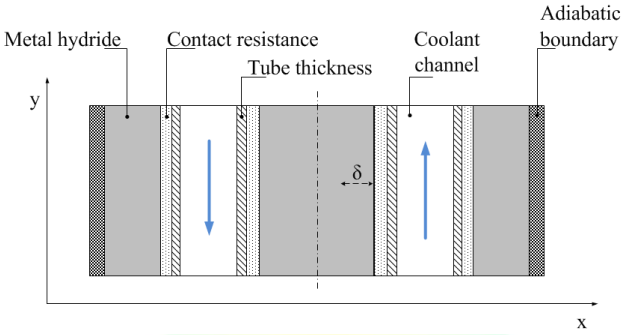

Figure 1. Bed domain considered for discretization.

Heat transfer is only permitted along the x axis wherein the entire solid enters into contact with the hydrogen at the same time and the heat generated from the absorption reaction is removed by the coolant that flows in the embedded tubes. The heat transferred between the solid and coolant occurs through the metallic thickness of the tube and a contact resistance. A value of 2000 mm^2/W for the contact resistance between solid and aluminum tubes has been considered [8].

The pressure ramp is 300 bar/min. Internal pressure rises from 1 bar to the desired value and is kept constant thereafter to study the temperature profile within the solid bed and the weight fraction of absorbed hydrogen at different distances from the cooling surface.

The coolant is Dexcool™, which is a typical anti-freeze car fluid. It is externally provided from the filling station during hydrogen charging. Its properties are reported in Table 1 for 0 °C, which is the temperature considered in the following analysis.

Table 1. Dexcool™ properties.

Temperature	**273 K**
Specific heat capacity, kJ/kg K^{-1}	3.46
Thermal conductivity, W/m K^{-1}	0.415
Density, kg/m^3	1060
Kinematic viscosity, m^2/s	$6.80x10^{-6}$

2.4. Model Description

The fueling model proposed in this study is introduced in the next sub-sections. It uses transient mass and energy balances along with a kinetics model to develop the time evolution of solid bed temperature, hydrogen mass flow rate and absorption rate. It can be applied to different metal hydrides by substituting their properties values and modifying, if needed, the kinetic equation. Real gas equations and properties as a function of pressure and temperature are implemented for the hydrogen gas. At first, the results obtained from the model developed with constant MH parameters are discussed and compared to what presented in ref. [8], where a similar analysis was carried out. Later, the same model is simulated by implementing the variation of the effective thermal conductivity and specific heat capacity with pressure, obtained from experimental data interpolation at the HSL.

2.4.1 Continuity Equation

The essential thermal masses involved in the model are the porous medium (being the absorbing alloy) and the hydrogen gas that flows into the system. The latter is partly stored in the absorbed phase and partly in gaseous phase in the pores (being the expansion volume). This means that the metal hydride system must be treated as a discontinuous medium.

In a typical refueling analysis one is only interested in the hydrogen mass that flows into the tank. The fuel input is thus considered as the accumulation rate in the mass balance. At each moment of the refueling process the internal hydrogen mass concentration is expressed as,

$$\dot{m}_{H_2} = \varepsilon \cdot V_{MH} \cdot \frac{d\rho_g}{dt} + (1-\varepsilon)\rho_s \cdot V_{MH} \frac{dw}{dt} \quad (1)$$

where the LHS is the hydrogen mass per unit time that flows into the tank. The first term in the right hand side (RHS) represents the rate of accumulated hydrogen in the gas phase and second term represents the rate of accumulation in the absorbed phase. The absolute porosity of the metal hydride is expressed with the term ε, while ρ_g, ρ_s, w, V_{MH} are the gas and solid densities, the weight fraction of hydrogen absorbed in the bed respectively and the MH volume.

2.4.2 Energy Balance

The energy balance is applied to the metal hydride control volume and the coolant passage. The pressure vessel is simply modeled as an adiabatic boundary to allow comparisons with the literature.

In porous packed beds the contact area between gas and solid phases is typically large enough to allow the use of a local thermal equilibrium assumption with a good grade of accuracy. This is especially valid when a large value for the porosity is considered, as it occurs in this study (i.e. 60%). The energy balance is obtained from its general form [16], and it is expressed in Eq. (2):

$$\frac{dH_{syst}}{dt} = \dot{m}_{H_2} h_{in} + V_g \frac{dp}{dt} + q \quad (2)$$

The RHS of the equation represents the inlet and outlet energy terms related to the hydrogen input mass rate, the compression heat $V_g \cdot dp/dt$ and the heat flow exchanged with the heat exchanger through the solid bed q.

For what afore explained and considering constant porosity and solid density, the left hand term (LHS) in Eq. (3) is expanded as follows:

$$\frac{dH_{syst}}{dt} = \rho_s V_s \frac{dh_s}{dt} + \rho_g V_g \frac{dh_g}{dt} + h_g V_g \frac{d\rho_g}{dt} + \rho_s V_s w \frac{dh_w}{dt} + \\ + \rho_s V_s h_w \frac{dw}{dt} \quad (3)$$

where the derivatives involve h_s, h_g and h_w, being the specific enthalpy for the absorbing alloy, and hydrogen in the gas and absorbed phases respectively.

Eq. (3) in its general form can be applied to both absorption and adsorption processes. With a constant heat of absorption and by using the continuity equation, it is possible to manipulate the volumetric energy balance and highlight the single coefficients of T, p and w, as:

$$\Phi = \left[(1-\varepsilon)\cdot \rho_s w c_{p_g} + \rho_{MH} c_{MH}\right] \quad (4.a)$$

$$\Lambda = \left[(1-\varepsilon) + \left((1-\varepsilon)\cdot \frac{\rho_s}{\rho_g} w + \varepsilon\right)\cdot \left(1-\alpha_g T_{MH}\right) - \varepsilon\right] \quad (4.b)$$

$$\Psi = (1-\varepsilon)\rho_s \frac{\Delta H_a}{MW_g} \quad (4.c)$$

$$\mathrm{I} = \frac{\dot{m}_{H_2}}{V_{MH}}(h_{in} - h) + q''' \quad (4.d)$$

Where ΔH_a, MW_g and h are the molar heat of absorption, the H_2 molar weight and the enthalpy of hydrogen in the pores respectively. The latter is calculated at the charging pressure p and temperature T_{MH}. The $\rho_{MH} c_{MH}$ term is the product of the packing density to the metal hydride specific heat capacity. The volumetric heat rate q''' transferred through the solid bed, has been modeled by means of the Fourier equation as,

$$q''' = k_{MH} \nabla^2 T_{MH} \quad (5)$$

where k_{MH} is the effective thermal conductivity of the metal hydride. With respect to Fig. 1, the heat is transferred from the solid through a series of thermal resistances, being the solid resistance itself, the contact resistance, the aluminum tube thickness and the convection resistance.

Finally, the temperature in the solid bed is calculated by means of Eq. (6),

$$\Phi \frac{dT_{MH}}{dt} = -\Lambda \frac{dp}{dt} - \Psi \frac{dw}{dt} + \mathrm{I} \quad (6)$$

2.4.3 Kinetic Equation

The kinetic model used in this study refers to the reaction parameters of $LaNi_5$ and is based on an expression for hydrogen absorption in the such metal hydride derived by Mayer et al. [17] that assumes first order kinetics, as it is often observed in metal hydrides. Indeed, a complete characterization of the kinetics of $Ti_{1.1}CrMn$ has not been reported in the literature, and hence, the reaction parameters such as activation energy, E_a and Arrhenius constant, C_a are unknown for such absorbing alloy. The kinetic model assumes the reaction parameters of $LaNi_5$ as reasonable engineering estimates for $Ti_{1.1}CrMn$ as it is typically done in the literature. The reaction rate of hydrogen per unit mass of metal hydride is expressed as,

$$\frac{dw}{dt} = C_a e^{E_a/(RT_{MH})} \ln\left(\frac{p}{p^{eq}}\right)\cdot (w_{\max} - w) \quad (7)$$

where p^{eq} is the equilibrium pressure of the MH and w_{max} is the maximum weight fraction of hydrogen absorbed in the bed. The absorption reaction proceeds only when $p > p^{eq}$.

The equilibrium pressure is a function of the metal hydride temperature and is given by the van´t Hoff equation:

$$p^{eq} = p_0 e^{\frac{\Delta H_a}{RT_{MH}} - \frac{\Delta S_a}{R}}$$

where p_0 and ΔS_a are the ambient pressure and the entropy of reaction respectively.

3. Results

3.1 Model with constant parameters.

At first the model is simulated with constant k_{MH} and c_{MH}, the nominal values of which are 1 W/m.K and 500 J/kg.K respectively. The behavior of the metal hydride at different locations from the cooling tube stresses the importance of the critical thickness concept, defined as the maximum distance from the cooling surface at which the reaction is completed below the desired filling time. In this study, a complete absorption is considered to be achieved at 80% of the MH saturation value (i.e. 1.5%) under a refueling time of 5 min.

In Fig. 2 (a) the volumetric heat generation rate is presented. It takes into account the heat of pressurization and the reaction heat in the solid bed. The reaction heat is a function of the absorption rate while the heat of pressurization is only function of the pressure ramp (and the porosity), which is positive and constant until the 300 bar condition is reached. For this reason, the heat of generation starts at a value different from zero and remains constant until the absorption reaction takes place. From the plot, two

points of maximum can be identified. One is a local maximum and occurs when the solid is affected by the cooling, which reduces the equilibrium pressure, enlarging the reaction driving potential and resulting in an increase in the reaction rate. The time at which this occurs depends upon the distance from the cooling surface and thus, upon the total thermal resistance of the local bed thickness.

The other is an absolute maximum, also named as the reaction peak.

At any distances the peak is observed at the end of the pressurization. The highest value is around 3.73 MW and corresponds to the highest cooling rate related to the solid in direct contact with the cooling surface. The peak decreases with the distance from the cooling element and remains nearly constant for the solid at a distance beyond 8 mm, as the thermal resistance is large enough to control the heat removal and thus, the absorption process. This can be seen also from Fig. 2 (b) where the reaction rate is plotted. The absorption rate presents similar values at the end of the pressurization for distances beyond 8 mm, and then start diverging due to the different cooling rates.

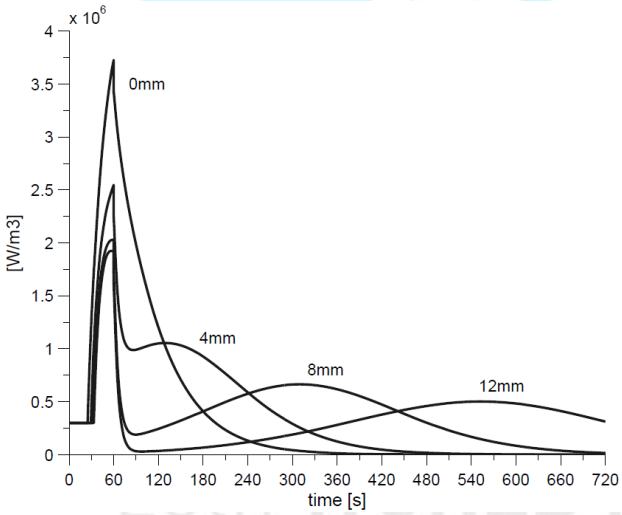

(a)

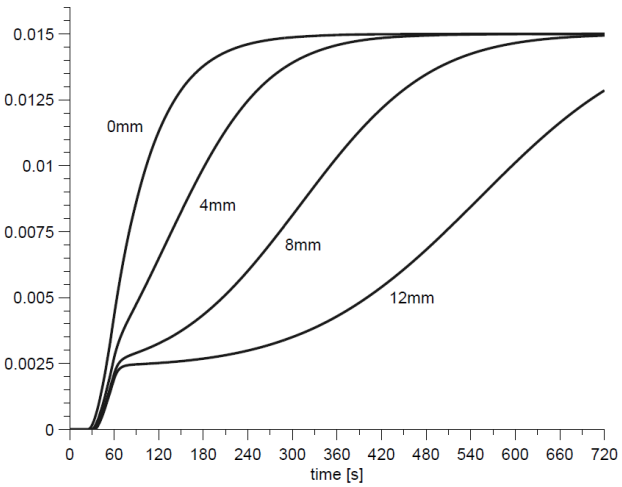

(b)

The reaction starts earlier for the solid closer to the coolant. For instance, at a location of 12 mm, the reaction does not start before 34 seconds, while the solid in direct contact with the tube starts reacting at 25 seconds. At such location the reaction proceeds smooth and no inflection in the curve can be detected at the end of the pressurization. It follows that the absorption process is kinetics limited. Only the reaction peak is present and no local maximum can be identified.

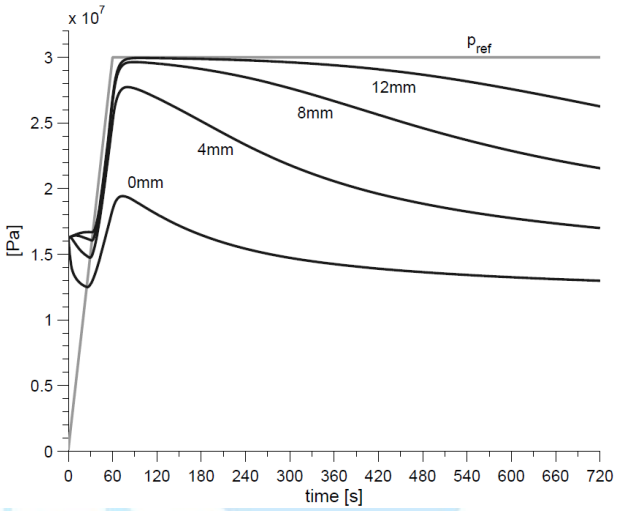

(c)

Figure 2. Heat generation rate per unit volume (a); weight fraction of absorbed hydrogen (b); equilibrium and charging pressures (c) at different locations.

In Fig. 2 (c) the equilibrium pressure is shown along with the pressure ramp, expressed in Pa. The solid thicknesses that experience higher reaction rates are related to larger difference between charging and equilibrium pressures for what above discussed.

These results are well aligned with what presented in ref. [8], and obtained by applying a simple heat transfer model to the same domain and metal hydride. In the same study, the critical thickness has been estimated to be around 10 mm under the same fueling conditions of current analysis.

3.2 Implementation of variable parameters in the model

To develop an efficient heat exchanger design for metal hydride storage applications, a detailed knowledge of the thermal properties is needed. Among these, thermal contact resistance, effective thermal conductivity and specific heat capacity play a major role in the absorption reaction and heat removal. In this study, the latter two parameters have been varied as functions of charging pressure and reaction progress to investigate the effect on the MH critical thickness. This is done by implementing interpolated experimental data in the 1D model. Measurements have

been carried out by Flueckiger et al. with the transient plane source method (TPS) at the Hydrogen Systems Laboratory at Purdue University and have been presented in detail in ref. [18].

The thermal contact resistance is maintained constant to its nominal value (2000 mm^2 K/W) for all simulations.

3.2.1 Effective thermal conductivity

For the activated $Ti_{1.1}CrMn$ powder, k_{MH} was measured to be 0.31 to 0.69 W/(m K) as a function of hydrogen pressure from 2.9 to 253 bar. The activation process reduces the particle size from 100 to 2-10 μm, constricting the solid conduction pathways, which in turn decreases the overall conductivity with respect to the oxidized powder. No significant dependency on hydrogen concentration was observed, and k_{MH} was dominated by the gaseous hydrogen pressure. For this reason, the thermal conductivity data are here interpolated as a function of the hydrogen charging pressure.

Although the experiments were conducted under similar filling conditions, as those considered in the current study, there are some differences that should be pointed out. Due to the commercial TPS system used, experiments in the hydriding region were not started until the temperature of the MH powder decreased to 16-18 °C (i.e. room temperature during measurements) in order to achieve accurate data acquisition. The higher metal hydride temperature (up to 55 °C), that results from the exothermic nature of the absorption process, is expected to increase k_{MH} to values in the neighborhood of 1 W/m.K. In addition, the greater packing densities considered in the simulation model with respect to measured samples, would further increase the effective thermal conductivity. However, despites of these observations, only the effect on δ that can be addressed to variable parameters that have been experimentally measured, is investigated and k_{MH} is assumed not to be influenced by temperature and bed porosity in the current analysis.

3.2.2 Effective specific heat capacity

At low pressures, the c_{MH} for activated $Ti_{1.1}CrMn$ powder was found to be lower than for oxidized powder. This can be addressed to the lack of oxidation layer in the particle surface. The specific heat was measured as a function of the hydrogen charging pressure. Below the hydriding region, the specific heat remains nearly independent of pressure and settles between 500-600 J/(kg K). A dramatic increase, up to 1050 J/(kg K) occurred at a charging pressure around 170 bar, as a result of the transition to the β–phase lattice structure and resulting phonon transport at the hydrogen occupied interstitials of the MH lattice. By relating the charging pressure and temperature to the hydrogen absorption, it was observed that such abrupt increase is a function of the reaction progress, F. The specific heat was found to vary with a smooth transition from desorbed phase to the full hydriding phase of the absorption process.

For this reason in the current study, c_{MH} data are interpolated as a function of the reaction progress variable, which is defined as,

$$F = \frac{w}{w_{\max}}$$

3.2.3 Effect on the metal hydride thickness

Measurements for k_{MH} and c_{MH} showed lower and greater values respectively, than in the nominal case. As a result, the temperatures in the solid bed are expected to increase for the combination of larger thermal resistances and inertia, that are attributed to the reduction in the conductivity and increase in heat capacity respectively. This can be seen in Fig. 3 (a), where the solid bed temperatures are plotted at different distances from the cooling surface for constant and variable MH parameters.

In the latter case, higher temperatures occur before and after pressurization. Indeed, larger thermal resistances decrease the cooling rates, while greater heat capacities reduce the speed of temperature response to the cooling rate. The increase in temperature is less important for thicknesses above 12 mm, as at this location the temperature reaches the adiabatic value of 55 °C at the end of pressurization.

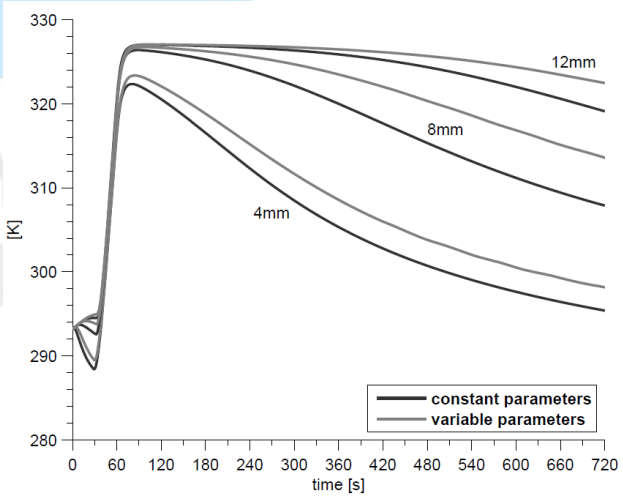

(a)

The effect of temperature on the reaction rate depends on the total thermal resistance between the solid powder and the coolant. This is evident when observing Fig. 3 (b), in which the weight fraction of hydrogen absorbed in the bed is shown.

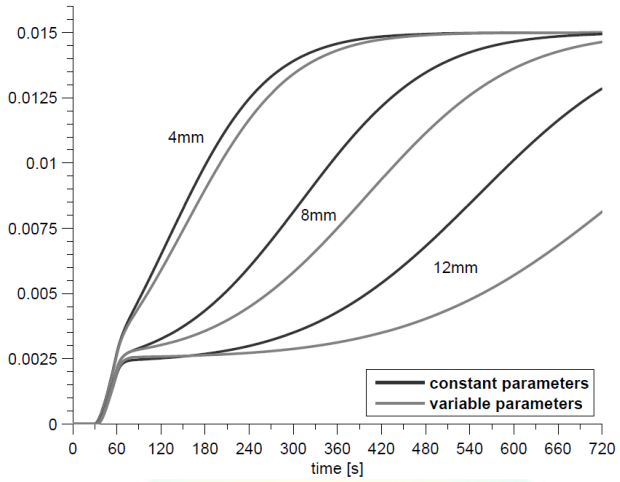

(b)

Figure 3. Temperature (a); weight fraction of hydrogen absorbed (b) in the bed. Effect of variable parameters.

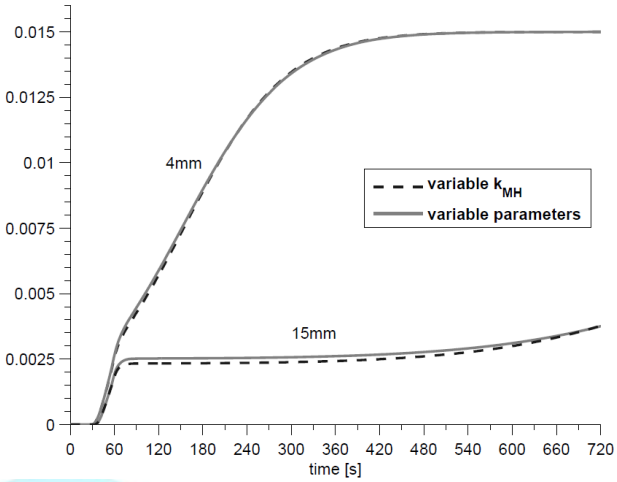

Figure 4. weight fraction of absorbed hydrogen for variable parameters and variable k_{MH} only.

At locations in close proximity to the cooling surface, the reaction is kinetics limited and a few degrees increase in temperature do not affect much the reaction rate, as the total thermal resistance is low enough to enable large cooling rates. The contrary occurs at further distances, at which the reaction is heat transfer limited.

Finally, with variable MH parameters, the metal hydride thickness reduces by nearly 1 mm, which corresponds to 10% of the value previously estimated for the nominal case with constant parameters. Thus for $Ti_{1.1}CrMn$, the variable parameters seem to have a non-significant effect on the estimation of the metal hydride thickness, which is the key criterion for the design of the heat exchanger.

The effect is expected to be negligible in practice, due to the positive influence of temperature increase on the enhancement of k_{MH} during exothermic absorption.

3.2.4 Influence of conductivity and specific heat capacity

The effect of k_{MH} and c_{MH} is separately investigated to study whether a predominant influence on the metal hydride thickness can be addressed to one of such parameters.

The model is modified to take into account only the dependency of the thermal conductivity upon the pressure, while the specific heat capacity is kept constant and equal to its nominal value. The former scenario is compared with the variable parameters case in Fig. 4 with respect to the weight fraction of absorbed hydrogen.

Two locations representative of small and large solid thicknesses are selected.

At 4 mm the curves are coincident. When a discrepancy is observed after pressurization, as at a distance of 15 mm, the effect of the specific heat capacity is a decrease in the reaction rate due to the higher temperature related to larger thermal inertia. However, such influence seems to be negligible on the weight fraction of absorbed hydrogen. It follows that the disparity in results observed in Fig. 3 should be addressed mainly to the lower values of thermal conductivities. The main reason for this is that c_{MH} varies with F more rapidly at locations in close proximity with the cooling surface, where the metal hydride experiences intensive cooling rates and is dominated by kinetics. As a result its effect on the reaction rate is negligible. On the contrary, at larger distances the large total thermal resistance strongly reduces the cooling rates, preventing the solid to achieve reaction rates high enough to trigger a significant variation in the c_{MH} value. At 15 mm and for a reaction time below 500s, the weigh fraction of absorbed hydrogen is 0.25% and the c_{MH} settles on a value around 550 J/kg.K, which is very close to its nominal value.

5. Conclusion

Thermal conductivity and specific heat capacity dependencies upon pressure and hydrogen content respectively, seem to have a small effect on the calculation of the critical metal hydride thickness for $Ti_{1.1}CrMn$. A constant-parameter 1D model describes the reaction rates and temperature distribution in the solid bed with a good grade of accuracy for the purpose of δ estimation. The difference in results for the critical metal hydride thickness was calculated to be 10%. This difference is to be addressed mainly to the lower thermal conductivity, while the specific heat capacity does not play a significant role. The increase of thermal conductivity that occurs in practice due to the

effect of temperature rise during absorption, is expected to reduce the difference in δ calculation to a negligible value.

Acknowledgements

The authors would like to thank the Danish Energy Agency for financial support, our industrial partner H2Logic and all the members of the Hyfill-Fast International Research Project for their collaboration. The authors would also like to thank Dr. Pourpoint and his team, at Purdue University, for the helpful insights and the courtesy of sharing their experimental data.

REFERENCES

[1] D. Mori et al. "High-pressure Metal Hydride Tank for Fuel Cell Vehicles," pp. 1–5, Jul. 2007.

[2] K. Toh et al. "Thermal Analysis of High-Pressure Metal Hydride Tank for Automotive Application," *MRS Symp. Proc.*, vol. 927, pp. 0927–EE01–07, Feb. 2011.

[3] N. Takeichi et al. "Application of hydrogen storage alloy at high pressure over 30 MPa," *Meet. Abstr. - 2004 Jt. Int. Meet. - 206th Meet. Electrochem. Soc.*, p. 549, 2004.

[4] B. Sakintuna et al. "Metal hydride materials for solid hydrogen storage: A review ☆," *Int. J. Hydrogen Energy*, vol. 32, no. 9, pp. 1121–1140, Jun. 2007.

[5] M. Raju et al. "System simulation model for high-pressure metal hydride hydrogen storage systems," *Int. J. Hydrogen Energy*, vol. 35, no. 16, pp. 8742–8754, Aug. 2010.

[6] T. L. Pourpoint et al. "Active cooling of a metal hydride system for hydrogen storage," *Int. J. Heat Mass Transf.*, vol. 53, no. 7–8, pp. 1326–1332, Mar. 2010.

[7] Y. Zheng et al. "Thermal management analysis of on-board high-pressure metal hydride systems," in *Proceedings of IMCE 2006 - ASME International Mechanical Engineering Congress and Exposition*, 2006, pp. 1–8.

[8] M. Visaria et al. "Study of heat transfer and kinetics parameters influencing the design of heat exchangers for hydrogen storage in high-pressure metal hydrides," *Int. J. Heat Mass Transf.*, vol. 53, no. 9–10, pp. 2229–2239, Apr. 2010.

[9] M. Visaria et al. "Enhanced heat exchanger design for hydrogen storage using high-pressure metal hydride: Part 1. Design methodology and computational results," *Int. J. Heat Mass Transf.*, vol. 54, no. 1–3, pp. 413–423, Jan. 2011.

[10] M. Visaria et al. "Coiled-tube heat exchanger for High-Pressure Metal Hydride hydrogen storage systems – Part 1. Experimental study," *Int. J. Heat Mass Transf.*, vol. 55, no. 5–6, pp. 1782–1795, Feb. 2012.

[11] M. Visaria et al. "Coiled-tube heat exchanger for high-pressure metal hydride hydrogen storage systems – Part 2. Computational model," *Int. J. Heat Mass Transf.*, vol. 55, no. 5–6, pp. 1796–1806, Feb. 2012.

[12] M. Visaria et al. "Enhanced heat exchanger design for hydrogen storage using high-pressure metal hydride – Part 2. Experimental results," *Int. J. Heat Mass Transf.*, vol. 54, no. 1–3, pp. 424–432, Jan. 2011.

[13] M. Visaria et al. "Experimental investigation and theoretical modeling of dehydriding process in high-pressure metal hydride hydrogen storage systems," *Int. J. Hydrogen Energy*, vol. 37, no. 7, pp. 5735–5749, Apr. 2012.

[14] "Dymola, Dynamic Modeling Laboratory - User´s Manual," *Dynasim AB*.

[15] Y. Kojima et al. "Development of metal hydride with high dissociation pressure," *J. Alloys Compd.*, vol. 419, no. 1–2, pp. 256–261, Aug. 2006.

[16] R. B. Bird et al. *Transport phenomena*, 2nd ed. New York (USA): John Wiley & Sons, 2002, p. 335.

[17] U. Mayer et al. "Heat and mass transfer in metal hydride reaction beds: experimental and theoretical results," *J. Less Common Met.*, vol. 131, pp. 235–244, 1987.

[18] S. Flueckiger et al. "In situ characterization of metal hydride thermal transport properties," *Int. J. Hydrogen Energy*, vol. 35, no. 2, pp. 614–621, Jan. 2010.